RESEARCH ARTICLE

Energy-Saving Algorithm Considering Cornering Resistance of a Four-Wheel Independent Drive Electric Vehicle With Vehicle-to-Vehicle (V2V) Information

JUNG HYUN CHOI[1], **(Member, IEEE), DOHEE KIM**[2], **(Member, IEEE), JEONG SOO EO**[2], **(Member, IEEE), AND SEHOON OH**[1], **(Senior Member, IEEE)**

[1]Department of Robotics and Mechatronics Engineering, Daegu Gyeongbuk Institute of Science and Technology (DGIST), Daegu 42988, South Korea
[2]Electrified Systems Control Research Laboratory, Research and Development Division, Hyundai Motor Company, Hwaseong 445-010, South Korea

Corresponding author: Sehoon Oh (sehoon@dgist.ac.kr)

ABSTRACT This study proposes an algorithm to save driving energy in an autonomous vehicle based on vehicle-to-vehicle technology. Saving the vehicular driving energy can be realized by reducing unnecessary deceleration and acceleration occurred in road congestion and by reducing the resistance caused by the internal factors of the vehicle. The algorithm proposed in this study defines cornering resistance, one of the internal resistance factors of a vehicle while driving, in terms of steering angle. Thereafter, the control inputs of a vehicle are adjusted to reduce the cornering resistance. In particular, because the target vehicle is to be a four-wheel independent drive vehicle, there are many control input values such as steering angle and yaw moment. To simultaneously obtain the desired driving performance and the minimized driving energy in such a vehicle environment, the control input values are optimally distributed by leveraging model predictive control (MPC). Moreover, a weighting factor for the MPC to yield appropriate control inputs is selected by considering the predefined cornering resistance. A simulation setup linked with CarSim-Simulink is established to verify the reduction of driving energy through the proposed algorithm. The simulation results evaluate the driving performance, driving safety, and energy-efficient driving in various driving scenarios.

INDEX TERMS Energy-saving driving, four-wheel independent drive EV, cornering resistance, model predictive control.

I. INTRODUCTION

Electric vehicles (EVs) are popular alternatives to intercombustion because of climate change owing to exhaust emissions and the depletion of fossil fuels. Because an electric motor drives an EV, faster response and higher accuracy in vehicle motion control than an intercombustion-based vehicle are well-known characteristics. [1], [2]. Based on this characteristic of the driving motor in the EV, studies have been conducted to improve the driving stability and performance as

The associate editor coordinating the review of this manuscript and approving it for publication was Christopher H. T. Lee.

well as extend the driving range. In particular, it is essential to study the energy-efficient driving of electric vehicles because of the high battery costs and charging times involved.

Existing energy-efficient driving technologies are developed in various ways. They can primarily be divided into cases of saving driving energy by using a technology that handles information outside the vehicle or analyzing internal factors of the vehicle.

First, in the case of using information outside the vehicle, studies have employed vehicle networks and communication technologies such as vehicle-to-vehicle (V2V) or connected and automated vehicles (CAVs) to extend the driving

J. H. Choi *et al.*: Energy-Saving Algorithm Considering Cornering Resistance of a Four-Wheel Independent Drive Electric Vehicle

IEEE *Access*

range. [3], [4], [5]. In this approach, the vehicle exploits information such as traffic lights, traffic congestion, or driving pattern information of the preceding vehicles. Based on the information, vehicles enable energy-saving driving by reducing unnecessary acceleration and deceleration. Furthermore, research utilizing such external information about vehicles has a synergy that enhances user convenience and saves driving energy as vehicle electronic communication-related technologies is becoming mature.

In contrast to using external information about the vehicle, an approach using the internal vehicle details has also been proposed by several researchers.

First, it considers the efficiency and loss of a vehicular electric driving motor [6], [7], [8]. The study used the fact that the output power and loss appear differently depending on the structural characteristics of the electric motor. In particular, there are many studies on properly distributing the driving force required for the vehicle to the front and rear wheels based on the efficiency map of the electric motor [9] [10], [11]. In these studies, a mathematical model of iron and copper losses was developed to calculate the driving energy loss accurately. Moreover, there has been a study on high energy efficiency by improving the power density in terms of the mechanical design of the synchronous motor for an electric vehicle [12]. Although the study based on the efficiency map was successfully applied to vehicles, it may not be easy to obtain a significant effect in the motor efficiency map using enhanced motor manufacturing technology. Another study related to vehicular driving motors to reduce the total energy consumption is the use of regenerative energy from the driving motor [13], [14], [15]. However, the study focused only on the amount of regenerative energy, without a detailed battery model. Regarding the implementation of battery storage and reuse, research related to battery models, such as the technology for state of charge, should be conducted in parallel.

Second, studies have been conducted to reduce the resistance, such as the rolling or cornering resistance generated by the vehicle's chassis. Cornering resistance is the resistance acting in the driving direction of the vehicle [16], [17]. This resistance arises from the tire and the ground owing to the kinematic characteristics of the steering system when the vehicle is driving in lateral motion. Unlike the rolling resistance, the cornering resistance does not always act on the vehicle but depends on the vehicle's driving direction. The fact that cornering resistance varies depending on the lateral motion, including the steering angle, is the starting point of this study. However, most studies on cornering resistance have focused on interpreting it. Although certain studies analyzed the driving energy of a vehicle according to the steering angle [18] and tire slippage energy [19], the cornering resistance was not considered in their approaches.

Therefore, this study proposes a driving control algorithm to improve the driving range by combining the cornering resistance with V2V technology. To this end, cornering resistance is first defined in terms of the control inputs. Then, the amount of control input is adjusted to reduce the predefined cornering resistance during driving using vehicle network technology. This differs from the conventional approach to using the cornering resistance [20] in terms of the optimization method.

The rest of this paper is structured as follows: Section II briefly describes the system of a four wheels driven (4WD) EV controlled by the proposed algorithm. Section III proposes the driving control algorithm. In particular, an MPC-based method was designed to properly distribute the control inputs considering cornering resistance. Several case studies that compare driving energy, driving performance, and driving constraints are presented in Section IV to verify the proposed algorithm. Section V concludes the paper.

II. STRATEGY OF ENERGY-SAVING DRIVING OF 4WD EV

Here, a concrete example of an effective driving scenario for the proposed algorithm is presented. The specific driving scenario may occur on a general road situation. Thereafter, a mathematical model for the energy inside the vehicle, specifically the cornering resistance, is derived along with the vehicle model.
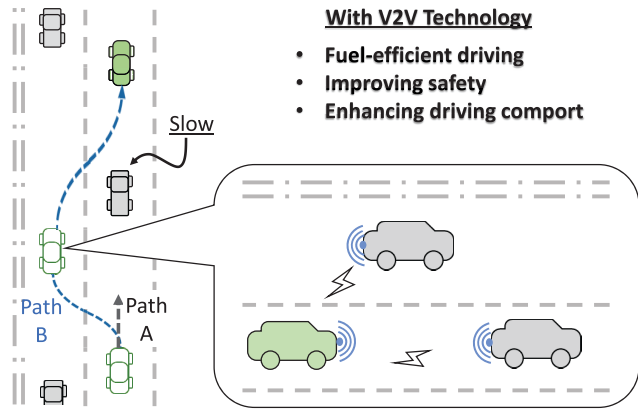
A. CONCEPT FOR ENERGY-SAVING DRIVING USING V2V TECHNOLOGY

To save driving energy, network technology between vehicles, such as V2V, is utilized. Figure 1 shows a specific driving scenario that compares the presence and absence of V2V technology in this study. The road congestion level assumed in this study corresponds to the C level of service (LOC) defined in the Highway Capacity Manual [21]. Vehicles may reduce the speed at the LOC C due to slight congestion, or lane changes may occur.

In Fig. 1, when driving without V2V technology, the driving path depends on the driver's vision information because the driver may only recognize the former vehicle situation. In this case, it is assumed that the driver may not know the entire vehicle situation on the road, such as congestion beyond the front vehicle. Consequently, the vehicle regulates its speed to maintain a safe stopping distance from the former vehicle, as shown in 'Path A' in Fig. 1. The speed pattern requires more driving energy for the vehicle and causes more traffic congestion on the road.

Conversely, when driving using V2V technology, the vehicle may drive with appropriate lane changes to avoid traffic jamming, such as 'Path B', as shown in Fig. 1. The driving route avoids unnecessary deceleration and acceleration of the vehicle, thereby saving driving energy and expecting a ride comfort effect. Moreover, the resistance element generated inside the vehicle should also be considered during lane-changing driving to minimize the driving energy.

A typical resistance factor considered when turning a vehicle is the cornering resistance. Therefore, a mathematical model of the vehicle is necessary to analyze the cornering resistance during turning.

IEEEAccess

J. H. Choi *et al.*: Energy-Saving Algorithm Considering Cornering Resistance of a Four-Wheel Independent Drive Electric Vehicle

FIGURE 1. Autonomous driving using V2V Technology. The road congestion level assumed corresponds to C level of service (LOC) defined in the Highway Capacity Manual [21].

B. MATHEMATICAL MODEL OF THE 4WD EV

The vehicle model for the proposed algorithm is a 4WD EV. The 4WD EV is expressed as a bicycle model, as shown in Fig. 2. Longitudinal motion is expressed in (1).

$$Ma_x = F_d - F_{CR} - B_1 v, \qquad (1)$$

where M is the mass of the vehicle, F_d is the driving force about the x-axis of the vehicle generated by the four wheels, respectively. F_{CR} is cornering resistance; B_1, and v are the coefficient of driving resistance and vehicle speed, respectively. Driving resistance, $B_1 v$ in (1) including the air resistance and tire rolling resistance, is assumed the only function of the vehicle speed for simplifying the equation.

The lateral and yaw motion dynamics can be derived by referring to the fundamental vehicle dynamics [22] as follows:

$$Ma_y = Mv(\dot{\beta} + \gamma) = F_f^y + F_r^y, \qquad (2)$$
$$I\dot{\gamma} = l_f F_f^y - l_r F_r^y + M_z, \qquad (3)$$

where M_z is the yaw moment generated by different driving forces on the right and left wheels [23]. I is the yaw inertia moment at the center of mass (CoM) of the vehicle. l_f and l_r are the distances from the CoM to the front and rear axles, respectively; F_f^y and F_r^y are the lateral forces of the front and rear wheels, respectively. Usually, it can be assumed that the left and right lateral forces on the front wheels are equal, and thus for the rear wheels. Let the sideslip angle, β, and yaw rate, γ, represent the state variables. Therefore, the lateral acceleration, a_y, can be assumed as $a_y = v(\dot{\beta} + \gamma)$ using the kinematic relationship. According to tire dynamic in [22], the lateral force consists of the cornering stiffness and side slip angle of the tire, and it is summarized as $F_i^y = -C_i \beta_i$, $i =$front, rear. Additionally, the sideslip angle of each wheel can be expressed as $\beta_f = \beta + l_f \gamma / v - \delta$, $\beta_r = \beta - l_r \gamma / v$. Thus, (2) and (3) can be rewritten as follows:

$$M\dot{\beta} = -\frac{C_f + C_r}{v}\beta - \frac{l_f C_f - l_r C_r + Mv^2}{v^2}\gamma + \frac{C_f}{v}\delta, \quad (4)$$
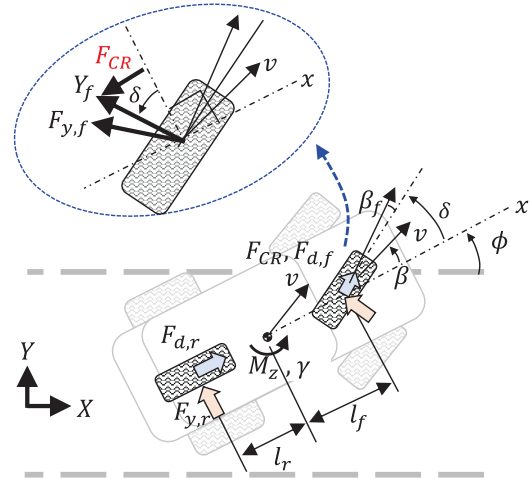
FIGURE 2. Schematic of a 4WD EV. Cornering resistance can be simplified as a function of steering angle.

$$I\dot{\gamma} = -(l_f C_f - l_r C_r)\beta - \frac{l_f^2 C_f + l_r^2 C_r}{v}\gamma \\ + l_f C_f \delta + M_z, \qquad (5)$$

where C_f and C_r are the combined cornering stiffness of the font and rear wheels, respectively; δ is the front steering angle. In (1), the cornering resistance F_{CR} appears during the cornering driving motion. As shown in the upper part of Fig. 2, F_{CR} can be simplified as the lateral force projected onto the longitudinal direction (x-axis) by the steering angle. That is, we have

$$F_{CR} = F_f^y \cos \beta_f \delta \approx F_f^y \delta, \qquad (6)$$

By substituting (6) into (1), the longitudinal motion equation can be rewritten as (7).

$$Ma_x = M\dot{v} = F_d - F_f^y \delta - B_1 v. \qquad (7)$$

The lateral kinematics Y of the vehicle is formulated as follows:

$$\dot{Y}_l = v\phi + v\beta, \qquad (8)$$

where the heading angle ϕ is assumed to be a small value for linearization. Based on (4), (6), (7), and (8), the state equation is constructed with the state, $\mathbf{x} = [x_d, Y_l, \phi, v, \beta, \gamma]^T$ as follows, where x_d and Y_l are the longitudinal and lateral travel distance, respectively. In addition, the driving force F_d, steering angle δ, and yaw moment M_z are adopted as input u.

$$\dot{\mathbf{x}} = \mathbf{A}\mathbf{x} + \mathbf{B}u, \qquad (9)$$
$$y = \mathbf{C}\mathbf{x}, \qquad (10)$$

J. H. Choi et al.: Energy-Saving Algorithm Considering Cornering Resistance of a Four-Wheel Independent Drive Electric Vehicle

IEEE Access

TABLE 1. Specification of the 4WD.

Specifications	value
Weight M	2270 kg
Inertia I	290 kgm^2
Distance from CG-Front wheel l_f	1.5 m
Distance from CG-Rear wheel l_r	1.6 m
Tire radius r_w	0.25 m
Front cornering stiffness C_f	110 kN/rad
Rear cornering stiffness C_r	120 kN/rad

where,

$$A = \begin{bmatrix} 0 & 0 & 0 & 1 & 0 & 0 \\ 0 & 0 & v & 0 & v & 0 \\ 0 & 0 & 0 & 0 & 0 & 1 \\ 0 & 0 & 0 & -\frac{B_1}{M} & 0 & 0 \\ 0 & 0 & 0 & 0 & \frac{(-C_f-C_r)}{Mv} & \frac{(-l_fC_f+l_rC_r-Mv^2)}{Mv^2} \\ 0 & 0 & 0 & 0 & \frac{(-l_fC_f+l_rC_r)}{I} & \frac{-l_f^2C_f-l_r^2C_r}{Iv} \end{bmatrix},$$

$$B = \begin{bmatrix} 0 & 0 & 0 \\ 0 & 0 & 0 \\ 0 & 0 & 0 \\ \frac{1}{M} & \frac{C_f\beta_f}{M} & 0 \\ 0 & \frac{C_f}{Mv} & 0 \\ 0 & \frac{l_fC_f}{I} & \frac{1}{I} \end{bmatrix}, \quad C = I_{6\times6}.$$

The specification of the 4WD vehicle is summarized in the Table. 1.

III. ENERGY-SAVING DRIVING ALGORITHM
A. OVERALL STRUCTURE OF THE CONTROLLER
The overall driving control algorithm for the 4WD EV is proposed, as shown in Fig. 3.

First, the "High-Level Controller" determines the lane change of the vehicle using information such as the speed of ahead vehicles and traffic jams from V2V technology. Thereafter, while the driving vehicle still has a certain speed, the lane change information, that is, the lateral movement distance, Y_l^*, and the heading angle, ϕ^* of the vehicle are provided to the optimal reference generator. Once "High-Level Controller" provides the lateral information of the vehicle for a lane change, the "Optimal Reference Control" calculates F_d, δ, and M_z to achieve the given lateral distance and speed. Notably, M_z, can be used as an extra input for the yaw motion of the vehicle through the torque vectoring technique [24]. Torque vectoring is essential for each wheel motor to realize the driving force and yaw moment because the vehicle proposed in this study is a 4WD independent drive type vehicle such as an actuated redundancy system [25]. Although there are many TV technologies [26], [27], in this study, the same quantity of torque was applied to each driving motor to achieve the given yaw moment and driving force for simplicity. In this way, the driving torque τ_i, where $i = 1, 2, 3, 4$, and δ are introduced into the vehicle system. Finally, the torque and angular velocity of each wheel ω_i, where $i = 1, 2, 3, 4$ are used to calculate the driving energy in
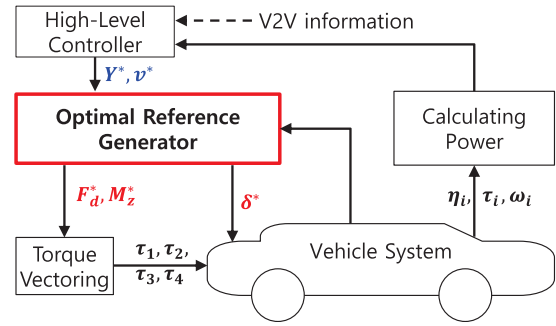

FIGURE 3. Overall driving control algorithm including optimal reference generator.

the "Calculating Power". The following equation calculates the driving energy E_a:

$$E_a = \int_0^{t_f} \eta T_i \omega_i \, dt, \tag{11}$$

where T_i and ω_i are the driving torque and speed of each wheel, respectively. t_f is the time required to conduct the simulation. For simplicity, the motor efficiency, η, is assumed as one for simplicity.

B. CONTROL INPUTS OPTIMIZATION WITH DRIVING CHARACTERISTIC CONSIDERATION
In this study, the travel trajectory and control input for the vehicle to achieve an optimized trajectory were optimized. Because the autonomous vehicle is the target vehicle, not only the motor torques but also the steering angle are considered as the control input to be optimized. That is, the optimal reference generator not only determines the reference path but also reduces the cornering resistance by optimally distributing the steering angle and yaw moment. According to (7), reducing the steering angle can mitigate the cornering resistance. In addition, the yaw moment as well as the steering angle affects the turning driving characteristics of a vehicle in the same way [22]. Therefore, if the yaw moment can compensate for the reduced steering angle completely, the cornering resistance can be reduced without deteriorating the driving performance. Moreover, in the case of deceleration, the yaw moment is related to the driving force; thus, it can save the driving energy.

In this study, MPC was used to consider various constraints of the vehicle system. The constrained optimization problem of MPC can be formulated by referring to a general form of the optimization problem [28] as follows:

$$\min J = \sum_{k=1}^{H_p} (\|x_k^* - x_k\|_Q^2 + \|u_{k-1}\|_R^2) \tag{12}$$

$$s.t \begin{cases} x_{k+1} = A_d x_k + B_d u_k, & k = 0 \ldots H_p - 1, \\ u_L \leq u_k \leq u_H, & k = 0 \ldots H_p - 1, \\ x_{\beta,L} \leq x_{\beta,k} \leq x_{\beta,H}, & k = 1 \ldots H_p, \\ x_{\gamma,L} \leq x_{\gamma,k} \leq x_{\gamma,H}, & k = 1 \ldots H_p, \end{cases} \tag{13}$$

where x_k for $k = 0, \ldots, H_p - 1$ are the predicted states within the prediction horizon H_p. In this study, a control horizon H_c

IEEE *Access*

J. H. Choi *et al.*: Energy-Saving Algorithm Considering Cornering Resistance of a Four-Wheel Independent Drive Electric Vehicle

$$J = \sum_{k=1}^{H_p} \left(\|x^* - x_k\|_Q^2 + \|u_{k-1}\|_R^2 \right)$$

$$= \sum_{k=1}^{H_p} \left(\|x^* - x_k\|_Q^2 + \left(R_1 F_{d,k-1} \right)^2 + (R_2 \delta_{k-1})^2 + \left(R_3 M_{z,k-1} \right)^2 \right)$$

$$= \sum_{k=1}^{H_p} \left(\|x^* - x_k\|_Q^2 + \underbrace{\left(v F_{d,k-1} \right)^2}_{\substack{\text{Longitudinal} \\ \text{motion power}}} + \underbrace{\left(F_f^y \delta_{k-1} v \right)^2}_{\substack{\text{Cornering} \\ \text{resistance}}} + \underbrace{\left(\gamma M_{z,k-1} \right)^2}_{\substack{\text{Yaw motion} \\ \text{power}}} \right)$$

$$R = \text{diag}(R_1, R_2, R_3), \qquad Q = \text{diag}(Q_1, Q_2, Q_3, Q_4, Q_5 Q_6)$$
$$\downarrow \ \downarrow \ \downarrow \qquad\qquad \downarrow \ \downarrow \ \downarrow \ \downarrow \ \downarrow \ \downarrow$$
$$F_d \ \delta \ M_z \qquad\qquad x_d \ Y_l \ \phi \ v \ \beta \ \gamma$$

FIGURE 4. Considerations for R, Q selection. In particular, the cornering resistance and yaw motion power are determined by proper R.
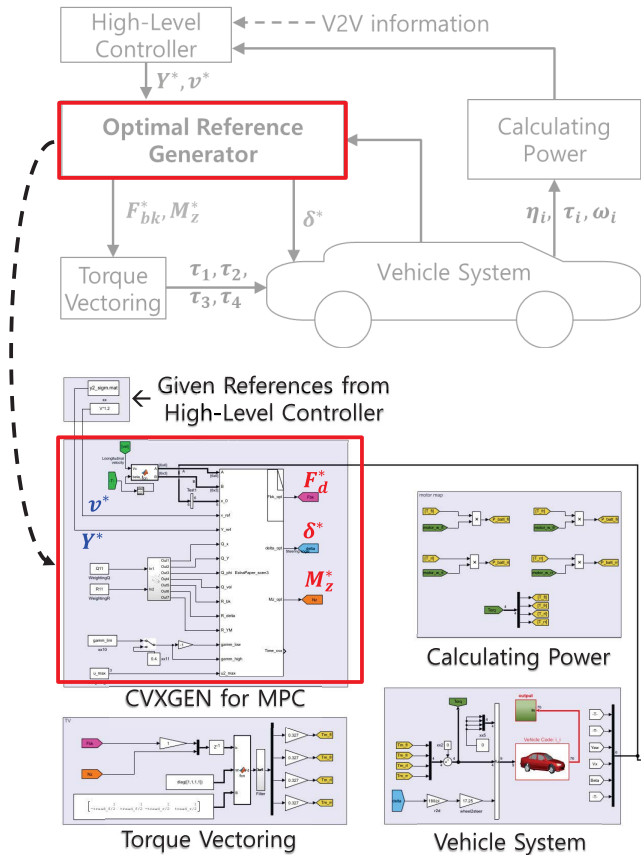
FIGURE 5. The simulation model for the optimal reference generator using MPC in CVXGEN [29].

is set as the same number as H_p. Thus, u_k for $k = 0, \ldots, H_p - 1$ corresponds to the predicted control sequence. In addition, A_d and B_d are the discretized matrices of A and B in (9) and can be approximated as follows.

$$\begin{cases} A_d = I + T_d A, \\ B_d = T_d B, \end{cases} \tag{14}$$

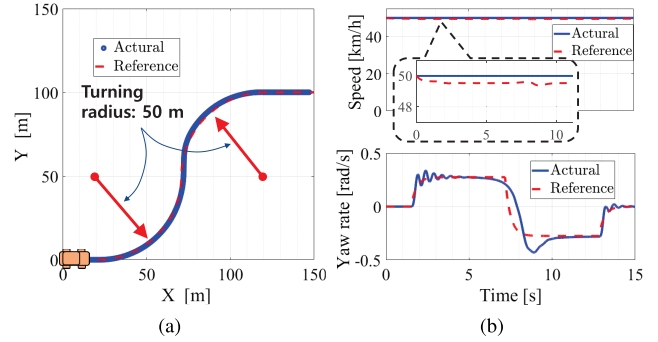where I is a 6-by-6 identity matrix and T_d is the sampling time.

FIGURE 6. Simulation result for circular driving test. (a) Vehicle trajectory. (b) Vehicle speed and yaw rate.

Since δ and M_z are used to generate a lateral motion, a guide to select R_2 and R_3 of the weighting factor R appropriately is needed. To choose the value of R_2, the cornering resistance power should be considered, as shown in Fig. 4. Similarly, the yaw motion power should be considered when selecting R_3. In general, R_2 is significantly larger than R_3 because of the physical properties of cornering resistance and yaw motion. Therefore, by referring to (7) and (6), R_2 and R_3 can be set as $R_2 = (F_f^y v)^2$ and $R_3 = \gamma^2$. To emphasize the reference tracking, we set $Q = \text{diag}(high, high, low, high, low, low)$, where the reference signals are: $x^* = [x_d; Y_l; \phi; 0; 0; 0]^T$.

In addition to minimizing the driving energy, the proposed algorithm considers constraints on the states and control inputs to ensure the driving performance and stability. That is, the constraints prevent the deterioration of the steering characteristic owing to distributed control inputs. Specifically, the maximum value of yaw rate x_γ was set not to exceed the range of neutral steering as follows.

$$-\gamma^* \leq x_{\gamma,k} \leq \gamma^*, \tag{15}$$

where γ^* is the desired yaw rate at the neutral steering condition as follows.

$$\gamma^* = \frac{v}{l}\delta. \tag{16}$$

The maximum value of side slip angle x_β was set for driving in a stable area as follows.

$$-\beta^* \leq x_{\beta,k} \leq \beta^*, \tag{17}$$

where β^* is the desired side slip angle at the neutral steering condition for the current steering angle. According to [22], β^* can be obtained as follows.

$$\beta^* = \left(1 - \frac{M}{2l}\frac{l_f v^2}{l_r Cr} \right)\frac{l_r}{l}\delta. \tag{18}$$

These two constraints guarantee performance and stability even when the yaw moment is applied to the vehicle using the optimization algorithm.
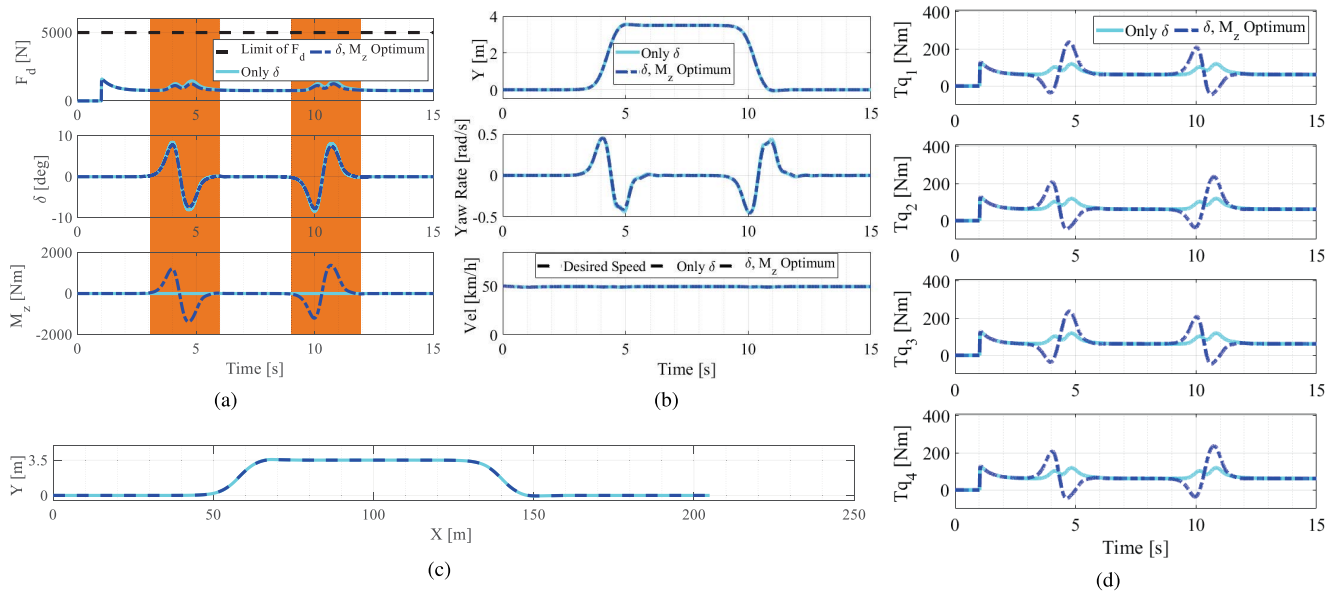
J. H. Choi *et al.*: Energy-Saving Algorithm Considering Cornering Resistance of a Four-Wheel Independent Drive Electric Vehicle

IEEE *Access*

FIGURE 7. Simulation results for driving scenario 2 with constant speed of the vehicle. The steering angle is reduced by 5.6% in this driving condition.
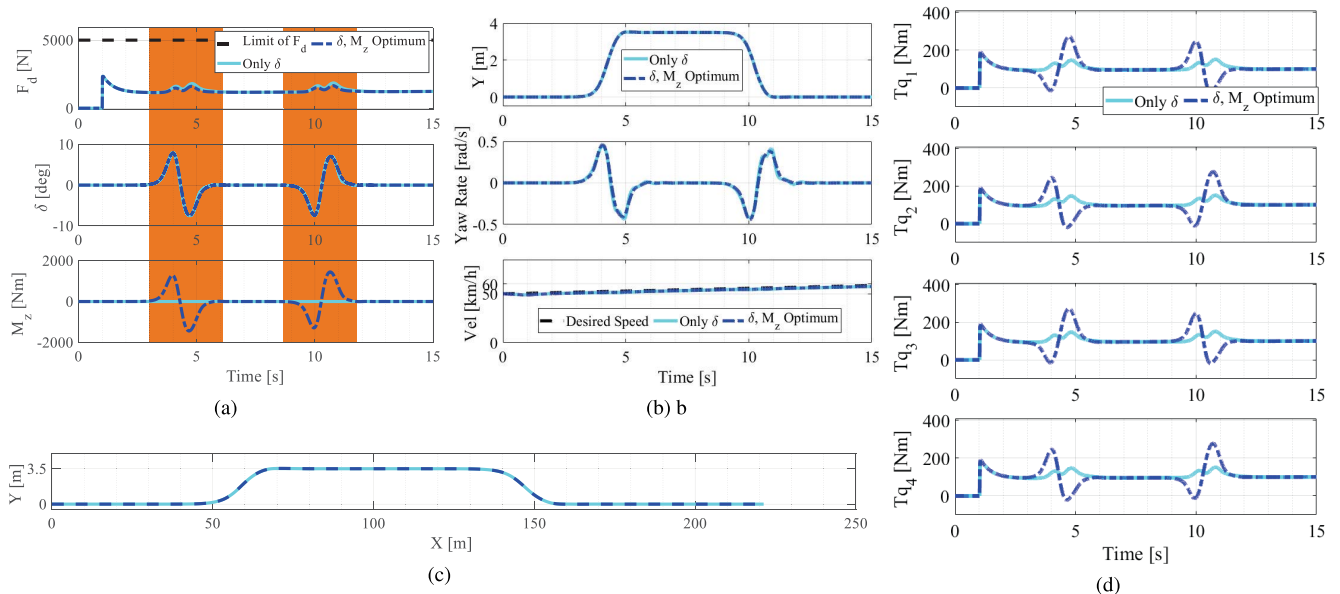

FIGURE 8. Simulation results for driving scenario 2 with acceleration motion of the vehicle. The steering angle is reduced by 0.7% in this driving condition.

IV. CASE STUDY WITH DRIVING SIMULATION

A. SIMULATION SETUP

Figure 5 shows the simulation setup used to implement the proposed algorithm. In the simulation, CarSim represented the vehicle model, and the CVXGEN-based S-function builder was applied to realize the MPC formulation. CVX-GEN employs an interior-point method and it is well known as a QP solver for numerical optimization problems. This simulation setup assumes that references Y_l, ϕ are obtained from the "Upper-Level Controller". Thereafter, the optimal F_d, δ and M_z can be calculated using the S-function builder for CVXGEN in the Fig. 5.
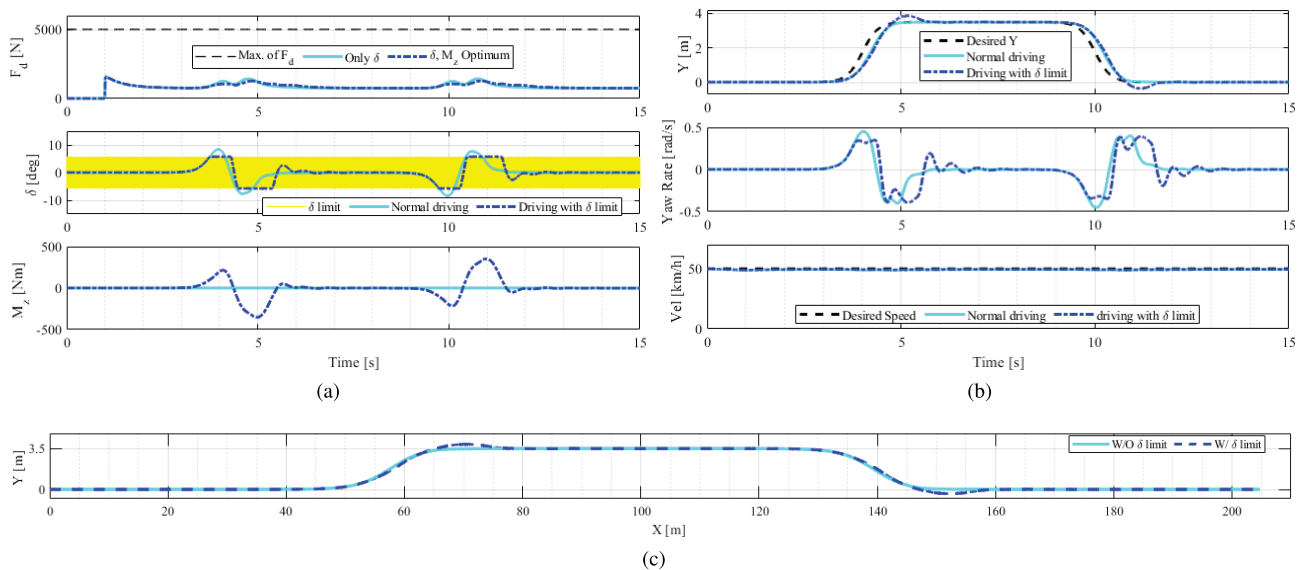
B. SIMULATION RESULTS

The proposed energy-saving algorithm is verified using three driving scenarios.

First, the driving performance of the proposed algorithm is demonstrated. The key idea of the proposed algorithm is that the optimal control input, steering angle, and yaw moment are regulated to mitigate the cornering resistance when the lane changes. The regulated input, for example, the steering angle, may imply deterioration in the driving performance. Therefore, a driving test was conducted on a road with a double quad arc with a radius of 50 m and the required driving performance was confirmed.
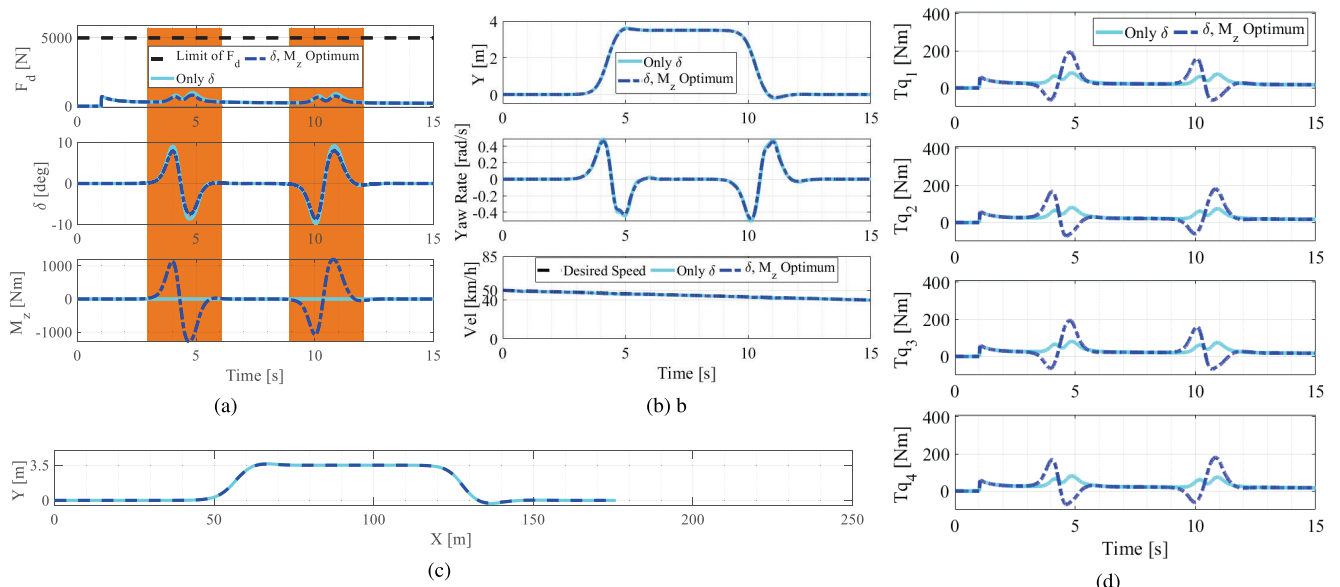
FIGURE 9. Simulation results for driving scenario 2 with deceleration motion of the vehicle. The steering angle is reduced by 11.5% in this driving condition.

FIGURE 10. Simulation results with δ limitation. (a) Control inputs. It is assumed that the steering angle (δ) has limited range with -0.1 < δ < 0.1 rad($\approx$ 5.7 degrees). (b) states of the vehicle system. (c) Comparison of vehicle trajectory.
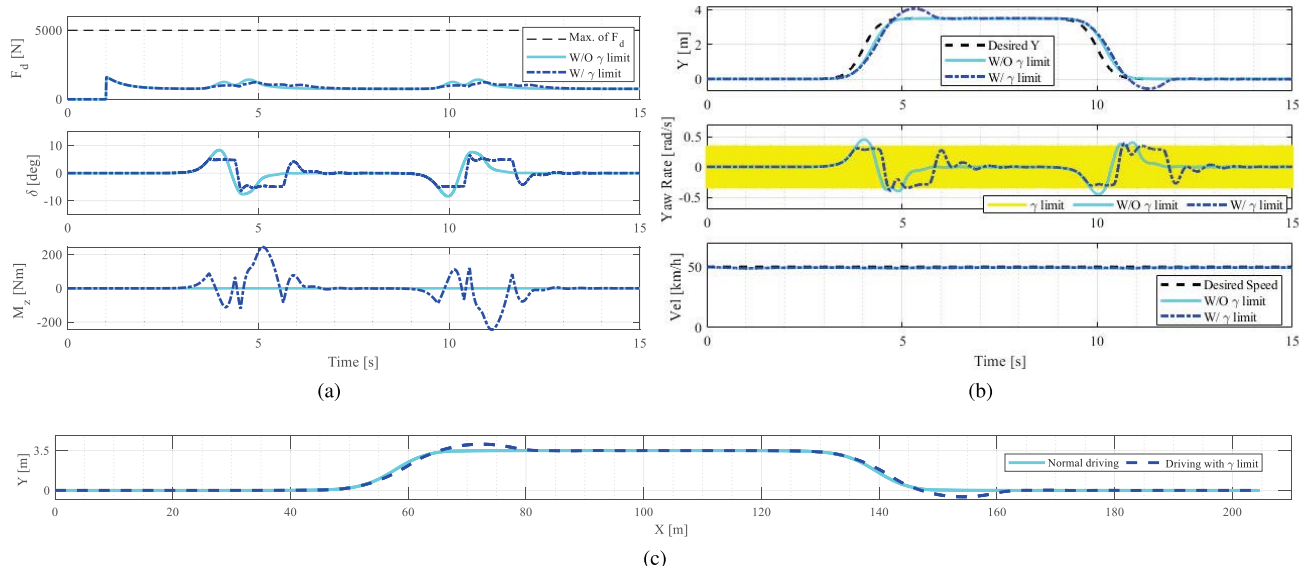
Second, the driving energy was compared and verified by the performance of the proposed algorithm. Therefore, the driving energy consumption was compared to the double-lane change. In particular, the vehicle speed under the test condition was not limited to a constant speed. The speed conditions, including acceleration/deceleration, were set to various values.

The third driving scenario is to certify the driving ability under internal constraints such as state and control inputs. This study applied MPC to distribute the steering angle and yaw moment to the optimal values in a given constraint situation. Therefore, it is necessary to check whether energy-saving algorithm is possible even when constraints change.

The simulation results for each driving scenario described above are as follows. The weighting factors, $\boldsymbol{R}$ and $\boldsymbol{Q}$, without optimization of δ and M_z, were set as $\boldsymbol{R} = $ diag($17e4, 45e4, 1e9$) and $\boldsymbol{Q} = $ diag($12e2, 1e3, 1e - 5, 11e2, 1e - 5, 1e - 5$), and those with optimization of δ and M_z, were also set as $\boldsymbol{R} = $ diag($17e4, 65e4, 7e - 6$ and $\boldsymbol{Q} = $ diag($12e2, 1e3, 1e - 5, 11e2, 1e - 5, 1e - 5$). The consequential simulation results are illustrated in Fig. 7 - 11.

1) SCENARIO 1) DRIVING PERFORMANCE IN DOUBLE-QUAD ARC DRIVING

In this scenario, the vehicle is driven along a double-quad arc road with a turning radius of 50 m, as shown in Fig. 6 (a). The vehicle has a constant speed of 50 km/h during the

J. H. Choi *et al.*: Energy-Saving Algorithm Considering Cornering Resistance of a Four-Wheel Independent Drive Electric Vehicle

IEEE *Access*

FIGURE 11. Simulation results with γ limitation. (a) Control inputs. (b) states of the vehicle system. It is assumed that the yaw rate (γ) is restricted to a range with -0.35 < γ < 0.35 rad/s. (c) Comparison of vehicle trajectory.

driving, as shown in Fig. 6 (b). Although oscillation and overshoot occur when the turning direction of the yaw rate is changed (approximately 2, 9, and 13 s in Fig. 6 (b)), the overall driving performance is reasonable. Because the yaw rate was stable throughout the entire driving section, the mean error was below 0.3%. In addition, the driving trajectory has well tracked the given reference values with a mean error of less than 0.9%, as shown in Fig. 6 (a). In this scenario, it must have a substantial Y_l value to travel within a certain radius, which is a driving setting that violates (8) assumed in this study. The range of the Y_l value assumed in (8) is ±3.5 m, which satisfies the lane width of a standard road. The Y_l value set in this scenario is approximately 30 times higher than the standard set value. Even if the driving condition of the lateral motion does not consider the proposed algorithm, it can be viewed as an advantage of the proposed driving control algorithm to produce satisfactory results.

The driving test result in the double-quad arc driving scenario shows that the proposed algorithm can be applied to the lane change path and typical road environments with an s-shaped driving path. However, the driving results do not represent the driving performance in more diverse environments, such as those involving a uniform circular motion or J-turn. Nevertheless, it is worth noting that the results sufficiently satisfy the driving performance and achieve the goal of this study.

2) SCENARIO 2) ENERGY-SAVING DRIVING AT VARIOUS DRIVING SPEEDS

First, the case of the lane change at a constant speed is presented in Fig. 7. The driving force in Fig. 7 (a) is not significant and it appears to be sufficient to maintain a constant speed. In particular, lane changes occur at approximately 4 and 10 s, and subsequently, a change in the driving force

occurs. It should be noted that the change in the driving force is caused by several factors, such as cornering and rolling resistance. Moreover, the driving force changes during the lane change are different, as shown in Fig. 7 (a), with the solid cyan and dashed blue lines. This difference can be explained by the resistance force, as shown in (6), because the steering angle changes when the lane changes. Because this resistance decreases the vehicle speed, a changing driving force occurs when changing lanes to compensate for this. Therefore, in this scenario, two types of simulations are compared: 1) applying the proposed algorithm to reduce the resistance and 2) using a typical driving algorithm. First, in the case of a typical driving algorithm, the yaw moment is not generated when the lane changes, as shown in Fig. 7 (a) by the cyan solid line. This means that the lane change caused by the lateral motion depends solely on the steering angle. However, in the case of the proposed algorithm, the yaw moment appears instead of reducing the steering angle when the lane changes. This is because the algorithm reduces the steering angle, as defined in (6). Subsequently, the yaw moment emerges to compensate for the reduced steering angle to satisfy the lateral motion, target Y_l as shown in Fig. 7 (a) with a dashed blue line. From these results, it can be noted that there is no deterioration in driving performance even if the proposed algorithm is applied, such as comparing the yaw rate or the driving trajectory, as shown in Fig. 7 (b) and (c). The driving torque of each wheel is well distributed by the "Torque Vectoring" rule adopted in this study, as shown in Fig. 7 (d). The remaining cases with acceleration/deceleration conditions are presented in Fig. 8 and 9. The driving force during acceleration/deceleration increases/decreases to reach the corresponding speed. The other parts are similar to the results for the constant-speed case described above. Based on this, the driving energy consumed according to each speed pattern is presented in Table. 2.

IEEE *Access*

J. H. Choi *et al.*: Energy-Saving Algorithm Considering Cornering Resistance of a Four-Wheel Independent Drive Electric Vehicle

TABLE 2. Comparison of driving energy of the proposed algorithm. The energy was calculated using (11). The predefined simulation time, t_f, was set to 15 s.

Vehicle speed	W/O Proposed	W/ Proposed	Improvement
Constant speed	56.2 Wh	53.7 Wh	4.4%
Acceleration	89.8 Wh	87.2 Wh	2.9%
Deceleration	22.4 Wh	20.7 Wh	7.6%

The simulation results of the second driving scenario show how much driving energy the algorithm saves. In particular, the amount of energy saving was divided according to the driving conditions: constant speed, deceleration, and acceleration. According to Table 2, the energy saving achieved in the acceleration period is slightly less than that in the other two cases because the steering angle reduction is insignificant, as shown in Fig. 8 (a). In contrast, the energy saving achieved during the deceleration period is the greatest of all the cases. Note that this deceleration is not a sudden deceleration that requires a braking force. Saving driving energy for deceleration that requires a braking force is beyond the scope of this study.

3) SCENARIO 3) DRIVING TEST IN RESTRICTED VEHICLE CONDITIONS

The algorithm proposed in this study aims to lower the driving energy. In particular, to implement this, MPC, which derives an optimal value from multi-constraints, was applied. Therefore, in the final simulation, the driving performance was verified under various constraints to confirm the MPC performance adopted in this study. Therefore, first, a lane-change simulation is performed, assuming that the range of the steering angle is restricted, as shown in Fig. 10. Notably, the steering angle, might be limited owing to defection of the steering system or other reasonable failures of the chassis. In Fig. 10 (a), the yellow box indicates the range of the limited steering angle, and the steering angle generated during driving does not exceed the restricted value, as indicated by the cyan solid line. Although the steering angle is limited, an additional yaw moment is yielded to maintain the tracking performance for a given Y_l, as shown in Fig. 10 (a). Therefore, the overall trajectory of the vehicle is well followed without much deviation compared with the non-restricted case, as shown in Fig. 10 (c). Tracking performance is not guaranteed when all steering angles are restricted. The allowed restriction for steering angle was up to 10%, with a tracking error of less than 1.2% in the mean value.

The second constraint that can be applied is when the yaw rate, which is one of the vehicle states, is limited, as illustrated in Fig. 11. In this case, the allowable yaw rate is limited to 10% in Scenario 2, as shown in the yellow box in Fig. 11 (b). The yaw rate can be restricted because it can act as a factor that affects the feeling of difference in driving or riding comfort. As a result of the simulation, the yaw rate did not generally exceed the limited range, except for intermittently deviating from the restricted value owing to the error between the model in (9) and the used CarSim vehicle

model. In particular, the control input, steering angle, and yaw moment are adjusted to satisfy the driving trajectory at the limited yaw rate, as shown in Fig. 11 (a). The results of the driving trajectory are presented in Fig. 11 (c), with a mean error of less than 2.2% from the given reference. Therefore, despite the restricted control input and state of the vehicle, driving performance was maintained within mean errors of 1.2% and 2.2% compared to the reference value.

The results of the third driving scenario show that the algorithm proposed in this study can be applied even if the steering angle or yaw rate of a vehicle is limited. Of course, an excessively limited steering angle or yaw rate seriously affects driving performance and stability. Nevertheless, it can be confirmed that the proposed algorithm works within the allowable limited vehicle situation. The 10 % limit regarding the steering angle and yaw rate is a design requirement considered in this study. On the other hand, areas such as loss of significant functions due to severe damage to the vehicle require additional research and are beyond the focus of this study.

V. CONCLUSION

In this study, cornering resistance was derived by considering the steering angle to reduce the driving energy for 4WD independent driving EVs. In particular, the steering angle is reduced to minimize the cornering resistance, which leads to the deterioration of the driving performance. This study adopted a method that increases yaw moment to prevent deterioration in driving performance and reduce driving energy. A linear MPC was employed to properly distribute the steering angle and yaw moment, as well as satisfy the driving conditions. In the MPC, the weighting factors of R and Q were selected based on the cornering resistance model and yaw motion model to reduce the steering angle and generate the yaw moment appropriately. The simulation results indicate that the driving control algorithm proposed in this study saves driving energy in three speed patterns. In addition, it was verified through a double-arc driving scenario with a constant radius that even if the steering angle and yaw moment were adjusted, the driving performance was not significantly affected. Finally, in the limit situation of the control input and state of the driving vehicle, the proposed driving control algorithm overcomes this and it verifies that the given trajectory is satisfied. In future, various approaches that reduce the driving energy will be considered by leveraging motor power efficiency maps and multiple torque vectoring methods.

REFERENCES

[1] H. Jing, F. Jia, and Z. Liu, "Multi-objective optimal control allocation for an over-actuated electric vehicle," *IEEE Access*, vol. 6, pp. 4824–4833, 2018.

[2] C. Gan, J. Wu, Q. Sun, W. Kong, H. Li, and Y. Hu, "A review on machine topologies and control techniques for low-noise switched reluctance motors in electric vehicle applications," *IEEE Access*, vol. 6, pp. 31430–31443, 2018.

[3] Y. Ma and J. Wang, "Energetic impacts evaluation of eco-driving on mixed traffic with driver behavioral diversity," *IEEE Trans. Intell. Transp. Syst.*, vol. 23, no. 4, pp. 3406–3417, Apr. 2022.

[4] M. Barth and K. Boriboonsomsin, "Energy and emissions impacts of a freeway-based dynamic eco-driving system," *Transp. Res. D, Transp. Environ.*, vol. 14, no. 6, pp. 400–410, 2009.

J. H. Choi *et al.*: Energy-Saving Algorithm Considering Cornering Resistance of a Four-Wheel Independent Drive Electric Vehicle

IEEE *Access*

[5] O. Teichert, A. Koch, and A. Ongel, "Comparison of eco-driving strategies for different traffic-management measures," in *Proc. IEEE 23rd Int. Conf. Intell. Transp. Syst. (ITSC)*, Sep. 2020, pp. 1–7.

[6] Y. Chen and J. Wang, "Adaptive energy-efficient control allocation for planar motion control of over-actuated electric ground vehicles," *IEEE Trans. Control Syst. Technol.*, vol. 22, no. 4, pp. 1362–1373, Apr. 2014.

[7] K. Kwon, M. Seo, and S. Min, "Efficient multi-objective optimization of gear ratios and motor torque distribution for electric vehicles with two-motor and two-speed powertrain system," *Appl. Energy*, vol. 259, Feb. 2020, Art. no. 114190.

[8] J. Wang, S. Gao, K. Wang, Y. Wang, and Q. Wang, "Wheel torque distribution optimization of four-wheel independent-drive electric vehicle for energy efficient driving," *Control Eng. Pract.*, vol. 110, May 2021, Art. no. 104779.

[9] W. Sun, J. Rong, J. Wang, W. Zhang, and Z. Zhou, "Research on optimal torque control of turning energy consumption for EVs with motorized wheels," *Energies*, vol. 14, no. 21, p. 6947, Oct. 2021.

[10] H. Fujimoto and S. Harada, "Model-based range extension control system for electric vehicles with front and rear driving–braking force distributions," *IEEE Trans. Ind. Electron.*, vol. 62, no. 5, pp. 3245–3254, May 2015.

[11] X. Yuan and J. Wang, "Torque distribution strategy for a front- and rear-wheel-driven electric vehicle," *IEEE Trans. Veh. Technol.*, vol. 61, no. 8, pp. 3365–3374, Oct. 2012.

[12] H.-J. Park and M.-S. Lim, "Design of high power density and high efficiency wound-field synchronous motor for electric vehicle traction," *IEEE Access*, vol. 7, pp. 46677–46685, 2019.

[13] M. Gautam, N. Bhusal, M. Benidris, and P. Fajri, "A GA-based approach to eco-driving of electric vehicles considering regenerative braking," in *Proc. IEEE Conf. Technol. Sustainability (SusTech)*, Apr. 2021, pp. 1–6.

[14] D. Kim, J. S. Eo, and K.-K.-K. Kim, "Service-oriented real-time energy-optimal regenerative braking strategy for connected and autonomous electrified vehicles," *IEEE Trans. Intell. Transp. Syst.*, vol. 23, no. 8, pp. 11098–11115, Aug. 2022.

[15] D. Kim, J. S. Eo, Y. Kim, J. Guanetti, R. Miller, and F. Borrelli, "Energy-optimal deceleration planning system for regenerative braking of electrified vehicles with connectivity and automation," SAE Tech. Paper 2020-01-0582, 2020.

[16] Y. Ikezawa, H. Fujimoto, D. Kawano, Y. Goto, Y. Takeda, and K. Sato, "Range extension autonomous driving for electric vehicle based on optimal vehicle velocity profile in consideration of cornering," *Electr. Eng. Jpn.*, vol. 207, no. 1, pp. 43–54, Apr. 2019.

[17] C. J. J. Beckers, I. J. M. Besselink, and H. Nijmeijer, "Assessing the impact of cornering losses on the energy consumption of electric city buses," *Transp. Res. D, Transp. Environ.*, vol. 86, Sep. 2020, Art. no. 102360.

[18] C.-H. Wu, "Optimization of steering control to improve the energy consumption of internal combustion engine vehicles," *Heliyon*, vol. 5, no. 12, Dec. 2019, Art. no. e03056.

[19] J. Wang, S. Lv, N. Sun, S. Gao, W. Sun, and Z. Zhou, "Torque vectoring control of RWID electric vehicle for reducing driving-wheel slippage energy dissipation in cornering," *Energies*, vol. 14, no. 23, p. 8143, Dec. 2021.

[20] W. Sun, J. Wang, Q. Wang, F. Assadian, and B. Fu, "Simulation investigation of tractive energy conservation for a cornering rear-wheel-independent-drive electric vehicle through torque vectoring," *Sci. China Technol. Sci.*, vol. 61, no. 2, pp. 257–272, Feb. 2018.

[21] *Highway Capacity Manual HCM2010*, Transp. Res. Board, Nat. Res. Council, Washington, DC, USA, 2010, vol. 1207.

[22] M. Abe, *Vehicle Handling Dynamics: Theory and Application*. London, U.K.: Butterworth, 2015.

[23] K. Nam, H. Fujimoto, and Y. Hori, "Lateral stability control of in-wheel-motor-driven electric vehicles based on sideslip angle estimation using lateral tire force sensors," *IEEE Trans. Veh. Technol.*, vol. 61, no. 5, pp. 1972–1985, Jun. 2012.

[24] J. Wang and R. G. Longoria, "Coordinated and reconfigurable vehicle dynamics control," *IEEE Trans. Control Syst. Technol.*, vol. 17, no. 3, pp. 723–732, May 2009.

[25] H. Cheng, Y.-K. Yiu, and Z. Li, "Dynamics and control of redundantly actuated parallel manipulators," *IEEE/ASME Trans. Mechatronics*, vol. 8, no. 4, pp. 483–491, Dec. 2003.

[26] S. Harada and H. Fujimoto, "Range extension control system for electric vehicles during acceleration and deceleration based on front and rear driving-braking force distribution considering slip ratio and motor loss," in *Proc. 39th Annu. Conf. IEEE Ind. Electron. Soc. (IECON)*, Nov. 2013, pp. 6626–6631.

[27] C. Chatzikomis, M. Zanchetta, P. Gruber, A. Sorniotti, B. Modic, T. Motaln, L. Blagotinsek, and G. Gotovac, "An energy-efficient torque-vectoring algorithm for electric vehicles with multiple motors," *Mech. Syst. Signal Process.*, vol. 128, pp. 655–673, Aug. 2019.

[28] Y. Gao, A. Gray, J. V. Frasch, T. Lin, E. Tseng, J. K. Hedrick, and F. Borrelli, "Spatial predictive control for agile semi-autonomous ground vehicles," in *Proc. 11th Int. Symp. Adv. Vehicle Control*, no. 2, 2012, pp. 1–6.

[29] J. Mattingley and S. Boyd, "CVXGEN: A code generator for embedded convex optimization," *Optim. Eng.*, vol. 13, no. 1, pp. 1–27, 2012.

JUNG HYUN CHOI (Member, IEEE) received the B.S. and M.S. degrees in mechanical engineering from Yeungnam University, South Korea, in 2010 and 2013, respectively, and the Ph.D. degree from the Department of Robotics Engineering, Daegu Gyeongbuk Institute of Science and Technology (DGIST), Daegu, South Korea, in 2021.

From 2013 to 2016, he was a Researcher at the IoT and Robotics Research Division, DGIST. Since 2021, he has been a Postdoctoral Researcher at the DGIST. His research interests include the development of mobile robot control algorithms, mechanical design, and motion control.

DOHEE KIM (Member, IEEE) received the B.S. degree in natural sciences and the M.S. degree in astronomy and space science from Yonsei University, in 2006 and 2008, respectively, and the Ph.D. degree in mechanical and aerospace engineering from the University of Florida, in 2011. Since 2012, he has been a Senior Research Engineer with the Electrified Systems Control Research Laboratory, Hyundai Motor Company. He specializes in non-linear control, adaptive control, optimal control, and model predictive control with practical applications to electrified vehicles, spacecrafts, and robotics.

JEONG SOO EO (Member, IEEE) received the B.S. degree in electronics engineering from Korea University, in 1994, and the M.S. degree in electrical and computer engineering from The University of Texas at Austin, in 2005. In 1993, he joined Hyundai Motor Company, where he has been a Research Fellow with the Electrified Systems Control Research Laboratory, since 2019. His research interests include observer-based control, non-linear control, and optimal control for (P)HEV and EV, software testing method, and on-board diagnosis system for internal combustion engine.

SEHOON OH (Senior Member, IEEE) received the B.S., M.S., and Ph.D. degrees in electrical engineering from The University of Tokyo, Tokyo, Japan, in 1998, 2000, and 2005, respectively.

He was a Research Associate at The University of Tokyo, until 2012, a Visiting Researcher at The University of Texas at Austin, from 2010 to 2011, a Senior Researcher at Samsung Heavy Industries, and a Research Professor at Sogang University. He is currently an Associate Professor at the DGIST, Daegu, South Korea. His research interests include the development of force control for human-friendly motion control algorithms and assistive/exercise devices for people.

Dr. Oh received the Best Transactions Paper Award from the IEEE TRANSACTIONS ON INDUSTRIAL ELECTRONICS, in 2013.

● ● ●